

Charge-ordered ferromagnetic phase in manganites

Tran Minh-Tien

*Institute of Physics, NCST, P.O. Box 429, Boho, 10000 Hanoi, Vietnam,
Electrophysics Department, National Chiao Tung University, Hsinchu 300, Taiwan.*

A mechanism for charge-ordered ferromagnetic phase in manganites is proposed. The mechanism is based on the double exchange in the presence of diagonal disorder. It is modeled by a combination of the Ising double-exchange and the Falicov-Kimball model. Within the dynamical mean-field theory the charge and spin correlation function are explicitly calculated. It is shown that the system exhibits two successive phase transitions. The first one is the ferromagnetic phase transition, and the second one is a charge ordering. As a result a charge-ordered ferromagnetic phase is stabilized at low temperature.

PACS numbers: 71.27.+a, 71.28.+d, 75.30.-m

There has been much recent interest in the properties of doped manganese oxides $R_{1-x}A_xMnO_3$ (R =rare earth, A =Ca,Sr).^{1,2} These materials present a very rich phase diagram involving phases with spin, charge and orbital order. The physically relevant electrons in manganites are those from the Mn $3d$ levels, which are split by the cubic crystal field into triply degenerate t_{2g} levels and higher-energy doubly degenerate e_g levels. Electrons from the e_g levels are able to hop between Mn sites and form a conduction band. Electrons from the t_{2g} levels are localized. The itinerant electrons and local spins are correlated by the double-exchange (DE) mechanism.^{3,4} The main feature of the DE is a cooperative effect where the motion of an itinerant electron favors the ferromagnetic (FM) ordering of local spins and, vice versa, the presence of the FM order facilitates the motion of the itinerant electron. The DE model qualitatively describes some of the magnetic properties of manganites,^{2,5} and provides a well-established starting point toward comprehensive understanding of the phase diagram of manganites.

Recently experiments have shown that beside the FM order a charge order can exist in the manganites.^{6,7} The charge order exists in regions with no net magnetization and, surprisingly, can also occur in FM regions.⁷ Doping of A^{2+} ions creates Mn^{4+} holes in a Mn^{3+} background. The presence of two valence states Mn^{3+} and Mn^{4+} may lead the compounds to a charge-ordered (CO) state for appropriate doping. However, the DE model alone cannot explain the CO state which coexists in the FM phase. In principle, the nearest-neighbor Coulomb repulsion may stabilize a CO state. However, a large nearest-neighbor repulsion likely destabilizes the homogeneous FM state and may produce a checkerboard charge order in three directions.² Another possible mechanism for the CO phase stabilization is the coupling of itinerant electrons to the Jahn-Teller distortions. However, the electron Jahn-Teller phonon coupling can only stabilize a CO-FM state where the CO phase transition occurs before the FM transition.⁸ At half filling experiments have only observed a charge order below the FM transition temperature.^{2,7} Therefore the Jahn-Teller coupling is unlikely responsible for the appearance of the CO-FM state at least at half filling. In this paper we

present a possible alternative explanation for the CO-FM state in the manganites. The key idea is an interplay of the DE and randomness of the A-site substitution. The randomness is inevitably introduced by experiments. The importance of the randomness has been discussed both experimentally and theoretically.^{1,2} The randomness can substantially decrease the critical temperature of the FM transition.^{9,10,11} Here we will incorporate the randomness of A-site substitution into the DE model. For simplicity, we adopt the randomness by A-site substitution as a random local potential of the itinerant electrons, although the randomness may cause other effects, for instance, randomness of the hopping or exchange integral.¹² It is well known that the diagonal disorder with binary distribution can be modeled by the Falicov-Kimball (FK) model.¹³ Although the FK model is simple, it contains a rich variety of phases. In particular, it illustrates the disorder-order phase transition driven by electron interaction.^{14,15} Incorporating the diagonal disorder of the FK type into the DE model, one may expect that a disorder-order phase transition could present. When the phase transition occurs, a CO-FM phase may be stabilized at low temperature. In order to detect the phase transition we study the charge and spin response of system by using the dynamical mean-field theory (DMFT).¹⁶ The DMFT has extensively been used for investigating strongly correlated electron systems.¹⁶ Within the DMFT we explicitly calculate the charge and spin correlation function. We find that the system stabilizes a CO-FM state at low temperature.

The system which we study is described by the following Hamiltonian

$$H = -\frac{t}{\sqrt{d}} \sum_{\langle ij \rangle, \sigma} c_{i\sigma}^\dagger c_{j\sigma} - \mu \sum_{i\sigma} n_{i\sigma} - 2J_H \sum_i S_i^z s_i^z + E_w \sum_i w_i + U \sum_{i\sigma} n_{i\sigma} w_i, \quad (1)$$

where $c_{i\sigma}^\dagger$ ($c_{i\sigma}$) is the creation (annihilation) operator of an itinerant electron with spin σ at lattice site i ; t/\sqrt{d} is the hopping parameter of the itinerant electrons. Here we have rescaled the hopping parameter with the dimension

d of the system. S_i^z is the z component of local spin at lattice site i , and for simplicity, it takes two values ± 1 . $s_i^z = (n_{i\uparrow} - n_{i\downarrow})/2$, $n_{i\sigma} = c_{i\sigma}^\dagger c_{i\sigma}$, w_i is a classical variable that assumes the value 1(0) if site i is occupied (not occupied) by A ion. U is the disorder strength and is mapped onto the difference in the local potential which splits energetically favor of Mn^{3+} and Mn^{4+} ions. The expectation value $x = \sum_i \langle w_i \rangle / N$, (N is the number of lattice sites), corresponds to the concentration of unfavorable Mn^{4+} sites. The chemical potential μ controls the carrier doping, while E_w controls the fraction of the sites having the additional local potential. We shall use the condition $n + x = 1$, where $n = \sum_{i\sigma} \langle n_{i\sigma} \rangle / N$ is the electron doping. This condition determines E_w for each doping n . The third term of Hamiltonian (1) is the Hund coupling of itinerant and local electrons. For simplicity we only take into account the Ising part of the Hund coupling. This simplification does not allow any spin-flip processes, which can be important at low temperature where spin-wave excitations may govern the thermodynamics of the system. However, in the DE processes the spin of itinerant electron ferromagnetically aligns with the local spin, hence, the Ising part of the Hund interaction plays a dominant role. The DMFT calculations for the DE model with classical local spins show that the simplification of the Hund coupling does not change the self energy of the single-particle Green function.⁵ Moreover, within the DMFT the numerical results for quantum local spins do not show a significant difference from the ones for classical local spins.¹⁷ Thus, one expects that within the DMFT the simplification of the Hund interaction does not result in a serious backwardness. J_H is the strength of the Hund coupling, and in the following we will take the limit $J_H \rightarrow \infty$. The first three terms of Hamiltonian (1) constitute a simplified DE model. This simplified model captures the most essential ingredient of the DE processes. The last two terms of Hamiltonian (1) describe a binary randomness of the A-site substitution. They together with the hopping term form the FK model.¹³ It is well known that within the FK model the U term induces a disorder-order phase transition.^{14,15} At low temperature a checkerboard ordering phase is stabilized. Hence, the model (1) may display an interplay of the FM and CO phase.

We solve model (1) by the DMFT. The DMFT is based on the infinite-dimension limit. In the infinite-dimension limit the self energy is pure local and has no momentum dependence. The Green function of itinerant electrons satisfies the Dyson equation

$$G_\sigma(\mathbf{k}, i\omega_n) = \frac{1}{i\omega_n - \varepsilon(\mathbf{k}) + \mu - \Sigma_\sigma(i\omega_n)}, \quad (2)$$

where $\omega_n = \pi T(2n + 1)$, $\varepsilon(\mathbf{k}) = -2t \sum_{j=1}^d \cos(k_j)$, and $\Sigma_\sigma(i\omega_n)$ is the self energy. In the infinite-dimension limit the bare density of states of itinerant electrons becomes $\rho(\varepsilon) = \exp(-\varepsilon^2/t^2)/\sqrt{\pi}t$ and we take t as the unit of energy ($t = 1$). The self energy is determined by solving an effective single-site problem. The effective action of

this problem is

$$S_{\text{eff}} = \sum_\sigma \int d\tau d\tau' c_\sigma^\dagger(\tau) \left(\frac{\partial}{\partial \tau} \delta(\tau - \tau') + \Lambda_\sigma(\tau - \tau') \right) c_\sigma(\tau') \\ + \sum_\sigma \int d\tau c_\sigma^\dagger(\tau) (-\mu + U w - J_H \sigma S^z) c_\sigma(\tau) + E_w w,$$

where $\Lambda_\sigma(\tau)$ describes the effective medium. This effective single-site problem can exactly be solved. Indeed, the dynamics of the localized spin S^z and impurity w involved in the effective action are independent, hence, we could independently take the trace over S^z and w in calculating the partition function. This is similar to the DMFT solving of the FK model.¹⁸ We obtain the local Green function in the limit $J_H \rightarrow \infty$

$$G_\sigma(i\omega_n) = \frac{W_{0\sigma}}{Z_\sigma(i\omega_n)} + \frac{W_{1\sigma}}{Z_\sigma(i\omega_n) - U}, \quad (3)$$

where $Z_\sigma(i\omega_n) = i\omega_n + \mu - \Lambda_\sigma(i\omega_n)$, and

$$W_{\alpha\sigma} = \left\{ \sum_{\alpha'=0,1} \sum_{\sigma'} \exp \left[-\beta E_w (\alpha' - \alpha) \right. \right. \\ \left. \left. \sum_n \ln \left(\frac{Z_{\sigma'}(i\omega_n) - \alpha' U}{Z_\sigma(i\omega_n) - \alpha U} \right) \right] \right\}^{-1}$$

with $\alpha = 0, 1$. In taking the limit $J_H \rightarrow \infty$ in deriving Eq. (3) we must first renormalize the chemical potential $\mu \rightarrow \mu + J_H$. The self energy is determined by the Dyson equation for the effective single-site problem

$$\Sigma_\sigma(i\omega_n) = Z_\sigma(i\omega_n) - G_\sigma^{-1}(i\omega_n). \quad (4)$$

Within the DMFT, the local Green function must coincide with the single-site Green function of the original lattice, i.e.,

$$G_\sigma(i\omega_n) = \frac{1}{N} \sum_{\mathbf{k}} G_\sigma(\mathbf{k}, i\omega_n). \quad (5)$$

Eqs. (2)-(5) form the complete set of equations, which self consistently determine the self energy and Green function.

We are interested in calculating the charge (c) and spin (s) correlation function

$$\chi^{c(s)}(i, j) = \langle (\delta n_{i\uparrow} \pm \delta n_{i\downarrow}) (\delta n_{j\uparrow} \pm \delta n_{j\downarrow}) \rangle \quad (6)$$

in the homogeneous paramagnetic (PM) phase ($\delta n_{i\sigma} = n_{i\sigma} - \langle n_{i\sigma} \rangle$). In order to calculate the charge and spin response of system one has to introduce an external field into the Hamiltonian. The charge and spin correlation function can be obtained by differentiating the Green function respected to the external field, and then taking the zero limit of the field.¹⁸ Following the standard techniques,¹⁸ one can express the correlation functions in the terms of charge (c) and spin (s) susceptibility $\chi^{c(s)}(\mathbf{q}, i\omega_n)$ in momentum space

$$\chi^{c(s)}(\mathbf{q}) = -T^2 \sum_n \chi^{c(s)}(\mathbf{q}, i\omega_n). \quad (7)$$

The charge and spin susceptibility can be obtained by differentiation of the Green function.¹⁸ We obtain

$$\chi^{c(s)}(\mathbf{q}, i\omega_n) = \frac{2 + \sum_{\alpha=0,1} \left(\frac{\partial \Sigma(i\omega_n)}{\partial W_\alpha} \right)_{G, W_{1-\alpha}} \Gamma_\alpha^{c(s)}(\mathbf{q})}{[\chi_0(\mathbf{q}, i\omega_n)]^{-1} - \left(\frac{\partial \Sigma(i\omega_n)}{\partial G(i\omega_n)} \right)_W}, \quad (8)$$

where $\chi_0(\mathbf{q}, i\omega_n) = \sum_{\mathbf{k}} G(\mathbf{k} + \mathbf{q}, i\omega_n) G(\mathbf{k}, i\omega_n)$. The matrix $\hat{\Gamma}^{c(s)}(\mathbf{q})$ satisfies the following equation

$$\hat{B}^{c(s)}(\mathbf{q}) \hat{\Gamma}^{c(s)}(\mathbf{q}) = \hat{Q}^{c(s)}(\mathbf{q}), \quad (9)$$

where $\hat{B}^{c(s)}(\mathbf{q})$ and $\hat{Q}^{c(s)}(\mathbf{q})$ have the following elements

$$B_{\alpha\beta}^{c(s)}(\mathbf{q}) = \delta_{\alpha\beta} + \sum_n \frac{A_\alpha^{c(s)}(i\omega_n) \eta(\mathbf{q}, i\omega_n) G(i\omega_n) \left(\frac{\partial \Sigma(i\omega_n)}{\partial W_\beta} \right)_{G, W_{1-\beta}}}{1 - G^2(i\omega_n) \left(\frac{\partial \Sigma(i\omega_n)}{\partial G(i\omega_n)} \right)_W + \eta(\mathbf{q}, i\omega_n) G(i\omega_n)}, \quad (10)$$

$$Q_\alpha^{c(s)}(\mathbf{q}) = \sum_n \frac{A_\alpha^{c(s)}(i\omega_n) \left(G^2(i\omega_n) \left(\frac{\partial \Sigma(i\omega_n)}{\partial G(i\omega_n)} \right)_W - 1 \right)}{1 - G^2(i\omega_n) \left(\frac{\partial \Sigma(i\omega_n)}{\partial G(i\omega_n)} \right)_W + \eta(\mathbf{q}, i\omega_n) G(i\omega_n)} \quad (11)$$

with $\alpha, \beta = 0, 1$. In deriving Eqs. (9)-(11) we have used the standard conversion¹⁸ $[\chi_0(\mathbf{q}, i\omega_n)]^{-1} = [G_\sigma(i\omega_n)]^{-2} + \eta(\mathbf{q}, i\omega_n) [G_\sigma(i\omega_n)]^{-1}$, and introduced quantity $A_\alpha^{c(s)}(i\omega_n) = \delta W_{\alpha\uparrow} / \delta Z_\uparrow(i\omega_n) \pm \delta W_{\alpha\downarrow} / \delta Z_\downarrow(i\omega_n)$. In the infinite dimension limit all of the wave vector dependence of $\chi_0(\mathbf{q}, i\omega_n)$ and $\eta(\mathbf{q}, i\omega_n)$ include in the term $X(\mathbf{q}) = \sum_{j=1}^d \cos q_j / d$. Hence, the spin and charge correlation function only depend on momentum via $X(\mathbf{q})$. Each of the derivatives appearing in Eqs. (8)-(11) can directly be calculated from the DMFT solution of Eqs. (2)-(5). In such the way $\hat{B}^{c(s)}(\mathbf{q})$ and $\hat{Q}^{c(s)}(\mathbf{q})$ are calculable once the self-consistent equations of the DMFT are solved. Equation (9) reveals that $\hat{\Gamma}^{c(s)}(\mathbf{q})$ will diverge at a temperature where the determinant of $\hat{B}^{c(s)}(\mathbf{q})$ vanishes, while $\hat{Q}^{c(s)}(\mathbf{q})$ remains finite. This results in an

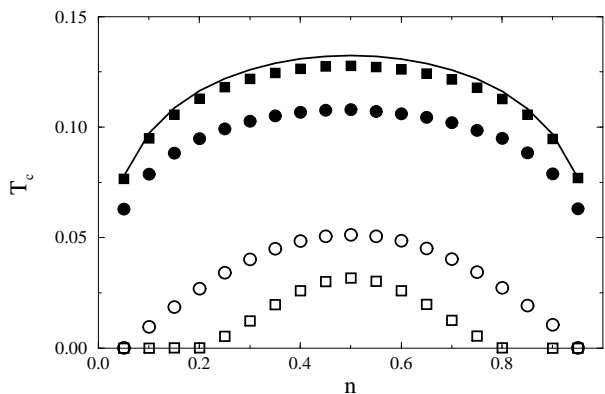


FIG. 1: The critical temperature T_c as a function of doping n for $U = 0.5$ (squares), $U = 1$ (circles). The filled (open) symbols are T_c of the FM (CO) phase transition. The solid line is T_c of the FM transition without disorder ($U = 0$).

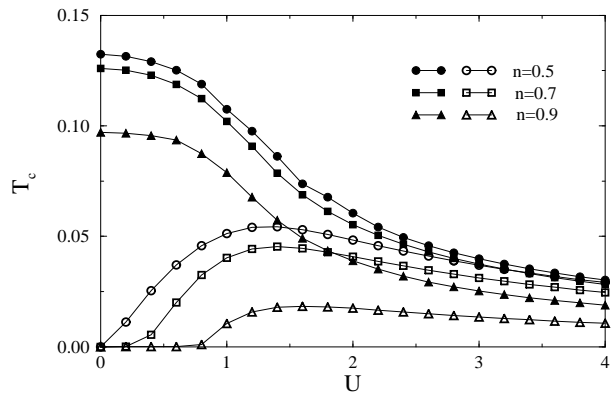


FIG. 2: The critical temperature T_c as a function of U for various doping n . The filled (open) symbols are T_c of the FM (CO) phase transition.

unphysical change of the sign of corresponding correlation function $\chi^{c(s)}(\mathbf{q})$ so that the assumption of the homogeneous PM phase fails for lower temperature. By a similar way one could also calculate the spin correlation function $\chi_S(\mathbf{q})$ of local spins. After some calculations we obtain

$$\chi_S(\mathbf{q}) = \gamma_0(\mathbf{q}) + \gamma_1(\mathbf{q}), \quad (12)$$

$$\sum_{\beta=0,1} B_{\alpha\beta}^s(\mathbf{q}) \gamma_\beta(\mathbf{q}) = \frac{2W_\alpha}{T}. \quad (13)$$

From Eqs. (9), (12)-(13) one can see that the spin correlation function of itinerant electrons and local spins will diverge at the same temperature where the determinant of $\hat{B}^s(\mathbf{q})$ vanishes. This means that the spin of itinerant electrons parallel aligns with local spin, and thus is an important feature of the DE. We calculate the charge and spin correlation function (7) by solving the DMFT set of self-consistent Eqs. (2)-(5). We are only interested in the FM and checkerboard CO phase stability. Hence, we only calculate the spin correlation function at $X_{\mathbf{q}} = 1$ and the charge correlation function at $X_{\mathbf{q}} = -1$. It is found that the spin correlation function $\chi^s(X_{\mathbf{q}} = 1)$ always diverges at a critical temperature. This is the signal of the FM phase transition. The charge correlation function $\chi^c(X_{\mathbf{q}} = -1)$ only diverges for $U \neq 0$. This means that without the disorder the system always is homogeneous. In Figs. 1 and 2 we present the critical temperature T_c of the FM and CO phase transition as a function of doping and disorder strength. At half filling $n = 0.5$ both critical temperatures reach their maximal value. The T_c of the FM transition always decreases with increasing disorder strength. This means that the disorder substantially decrease T_c of the FM transition.^{9,10,11} At the same time, with increasing U , T_c of the CO phase transition first increases, reaches its maximal value, and then decreases. The behavior of T_c of the CO phase transition is similar to the one in the FK model.¹⁸ At very strong disorder ($U \gg 1$) the two critical temperatures

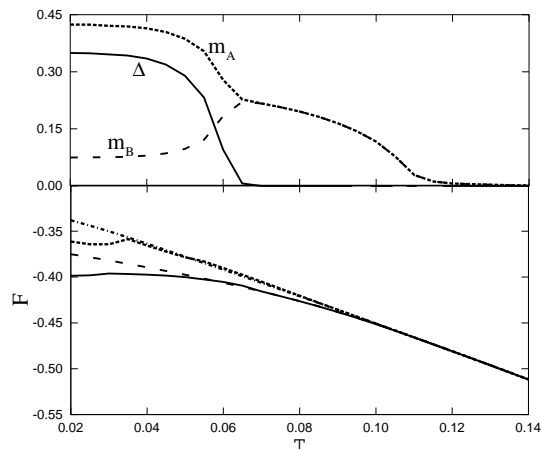


FIG. 3: Upper panel: the temperature dependence of the spin magnetization m_A (m_B) of sublattice A(B) (the dot and dashed line), and of the charge-order parameter Δ (the solid line).

Lower panel: the temperature dependence of the free energy F . The solid, long dashed, short dashed, and dot-dashed line are the free energy in the CO-FM, homogeneous FM, CO-PM, and homogeneous PM phase, respectively ($U = 1$, $\mu = U/2$).

approach to a same value. One also notices that T_c of the CO phase transition always is smaller than the FM transition temperature. Thus, one may expect that the CO state is stabilized in the FM phase at low temperature. However, this CO phase stability is respected to the homogeneous PM phase, and for safety we also study an inhomogeneous phase. We divide the lattice into two penetrating sublattices A and B . This lattice division allows us to study the checkerboard CO phase. By using the standard technique¹⁶ the matrix Green function can be written in the following form

$$\hat{G}_\sigma^{-1}(\mathbf{k}, i\omega_n) = \begin{pmatrix} i\omega_n + \mu - \Sigma_\sigma^A(i\omega_n) & -\varepsilon(\mathbf{k}) \\ -\varepsilon(\mathbf{k}) & i\omega_n + \mu - \Sigma_\sigma^B(i\omega_n) \end{pmatrix},$$

where $\Sigma_\sigma^{A(B)}(i\omega_n)$ is the self energy of the Green func-

tion of sublattice $A(B)$. The self energies are determined by solving the effective problem of single site of the sublattices.¹⁶ We find that at low temperature a checkerboard CO-FM state is stabilized. We plot the magnetization $m_{A(B)} = 2 \sum_{i \in A(B)} \langle s_i^z \rangle / N$ of sublattice A (B) as a function of temperature in Fig. 3 (upper panel). In this figure we also plot the temperature dependence of the charge-order parameter $\Delta = (\sum_{i \in A, \sigma} \langle n_{i\sigma} \rangle - \sum_{j \in B, \sigma} \langle n_{j\sigma} \rangle) / N$. It shows that below a critical temperature the magnetizations of both sublattices exist. They equal to each other until another critical temperature, where the charge-order parameter exists. At low temperature the system is in the checkerboard CO-FM state. In this phase the charge order coexists in the FM state, as experimentally observed.⁷ In the way the system exhibits two successive phase transitions. Initially the system goes to the homogeneous FM phase, and after that to the checkerboard CO phase, that the CO-FM phase is stabilized. We also calculate the free energy of the system. The free energy can only be expressed in terms of local quantities.¹⁶ We plot the temperature dependence of the free energy F in Fig 3 (lower panel). It shows that the CO-FM state has lowest free energy, hence the state must be stabilized at low temperature.

In conclusions, we have proposed a mechanism for the CO-FM phase which has recently been observed. The mechanism is based on a combination of diagonal disorder and a simple DE model with local Ising spins. Employing the DMFT we have calculated the charge and spin correlation function. It is found that the FM and CO state are stabilized at low temperature. As a result the checkerboard charge order can occur in the FM state. However, the manganites are too complicated a system to be completely described by this simple model. In particular, the phase with inhomogeneous percolation of FM and CO regions is beyond the scope of this paper.

This work was supported by the National Program of Basic Research on Natural Science of Vietnam, Project 4.1.2. The writing was completed at the National Chiao Tung University, and was supported by Project NSC 91-2811-M-009-006 of ROC.

¹ M. B. Salamon and M. Jaime, Rev. Mod. Phys. **73**, 583 (2001).

² E. Dagotto, T. Hotta, and A. Moreo, Phys. Rep. **344**, 1 (2001).

³ C. Zener, Phys. Rev. **82**, 403 (1951).

⁴ P. W. Anderson and H. Hasegawa, Phys. Rev. **100**, 675 (1955).

⁵ N. Furukawa, J. Phys. Soc. Jpn. **63**, 3214 (1994); *ibid.* **64**, 2754 (1995); *ibid.* **65**, 1174 (1996).

⁶ M. Uehara, S. Mori, C. H. Chen, and S.-W. Cheong, Nature **399**, 560 (1999).

⁷ J. C. Loudon, N. D. Mathur, and P. A. Midgley, Nature **420**, 797 (2002).

⁸ S. Yunoki, T. Hotta, and E. Dagotto, Phys. Rev. Lett. **84** 3714 (2000).

⁹ F. Zhong, J. Dong, and Z. D. Wang, Phys. Rev. B **58**, 15 310 (1998).

¹⁰ B. M. Letfulov and J. K. Freericks, Phys. Rev. B **64**, 174409 (2001).

¹¹ M. Auslender and E. Kogan, Phys. Rev. B **65**, 012408 (2001).

¹² J. Burgy *et al.*, Phys. Rev. Lett. **87**, 277202 (2001).

¹³ L. M. Falicov and J. C. Kimball, Phys. Rev. Lett. **22**, 997 (1969).

¹⁴ T. Kennedy and E. H. Lieb, Physica A **138**, 320 (1986); *ibid.* **140**, 240 (1986).

- ¹⁵ U. Brandt and R. Schmidt, Z. Phys. B **63**, 45 (1986); *ibid.* **67**, 43 (1987).
- ¹⁶ A. Georges, G. Kotliar, W. Krauth, and M. J. Rozenberg, Rev. Mod. Phys. **68**, 13 (1996).
- ¹⁷ K. Nagai, T. Momoi, and K. Kubo, J. Phys. Soc. Jpn. **69**, 1837 (2000).
- ¹⁸ U. Brandt and C. Mielsch, Z. Phys. B **75**, 365 (1989); *ibid.* **79**, 295 (1990), *ibid.* **82**, 37 (1991).